European Journal of Human Genetics (2015), 1–10

www.nature.com/ejhg

ARTICLE

A novel phenotype in N-glycosylation disorders: Gillessen-Kaesbach–Nishimura skeletal dysplasia due to pathogenic variants in ALG9

Emma Tham[1,2,12], Erik A Eklund[3,12], Anna Hammarsjö[1,2,12], Per Bengtson[4], Stefan Geiberger[5], Kristina Lagerstedt-Robinson[1,2], Helena Malmgren[1,2], Daniel Nilsson[1,2], Gintautas Grigelionis[1], Peter Conner[6,7], Peter Lindgren[6,7], Anna Lindstrand[1,2], Anna Wedell[1,8], Margareta Albåge[9], Katarzyna Zielinska[3], Ann Nordgren[1,2], Nikos Papadogiannakis[10,12], Gen Nishimura[11,12] and Giedre Grigelioniene*[,1,2,12]

A rare lethal autosomal recessive syndrome with skeletal dysplasia, polycystic kidneys and multiple malformations was first described by Gillessen-Kaesbach *et al* and subsequently by Nishimura *et al*. The skeletal features uniformly comprise a round pelvis, mesomelic shortening of the upper limbs and defective ossification of the cervical spine. We studied two unrelated families including three affected fetuses with Gillessen-Kaesbach–Nishimura syndrome using whole-exome and Sanger sequencing, comparative genome hybridization and homozygosity mapping. All affected patients were shown to have a novel homozygous splice variant NM_024740.2: c.1173+2T>A in the *ALG9* gene, encoding alpha-1,2-mannosyltransferase, involved in the formation of the lipid-linked oligosaccharide precursor of N-glycosylation. RNA analysis demonstrated skipping of exon 10, leading to shorter RNA. Mass spectrometric analysis showed an increase in monoglycosylated transferrin as compared with control tissues, confirming that this is a congenital disorder of glycosylation (CDG). Only three liveborn children with ALG9-CDG have been previously reported, all with missense variants. All three suffered from intellectual disability, muscular hypotonia, microcephaly and renal cysts, but none had skeletal dysplasia. Our study shows that some pathogenic variants in *ALG9* can present as a lethal skeletal dysplasia with visceral malformations as the most severe phenotype. The skeletal features overlap with that previously reported for ALG3- and ALG12-CDG, suggesting that this subset of glycosylation disorders constitutes a new diagnostic group of skeletal dysplasias.
European Journal of Human Genetics advance online publication, 13 May 2015; doi:10.1038/ejhg.2015.91

INTRODUCTION

Fetal skeletal dysplasias encompass a diverse group of disorders and the genetic causes are still unknown for a significant proportion of cases. A very rare lethal fetal syndrome with polycystic kidneys, typical facial features and varying malformations, was first reported by Gillessen-Kaesbach *et al*, while features of skeletal dysplasia in this syndrome were characterized by Nishimura *et al*.[1,2] Despite the varying degree and combination of internal malformations and dysmorphic features, the skeletal features of the patients were strikingly uniform, including short tubular bones, deficient ossification of the cervical vertebral bodies and pubic rami, round pelvis, decreased ossification of the frontoparietal bones, thickening of the occipital bones, ulnar deviation of the hands and short extremities.[1,2]

The congenital disorders of glycosylation (CDG) constitute a large group of syndromes with disruption of one or several of the biosynthetic pathways of complex glycans as a common denominator.[3] Most CDG patients have a disruption in the N-linked pathway, in which a lipid-linked precursor oligosaccharide (LLO), preformed in the endoplasmic reticulum (ER), is transferred to asparagine residues in the nascent polypeptide chain. CDG syndromes with disrupted N-linked glycosylation are multisystem disorders with, for example, intellectual disability, hypotonia, epilepsy, liver disease, coagulopathy, hormonal dysfunction and cardiac disease.[4] The severity varies greatly from mild intellectual disability with normal lifespan to neonatal lethality. Skeletal dysplasia is not a commonly recognized symptom of CDG syndromes but has been reported in rare patients.[5] Of note, a few patients with ALG3- and ALG12-CDG share some skeletal features with those described by Gillessen-Kaesbach *et al* and Nishimura *et al*.[1,2,6–8]

ALG9 encodes an alpha-1,2-mannosyltransferase that catalyzes two steps in the LLO biosynthesis. The biosynthesis starts on the cytosolic side of the ER where a dolichol pyrophosphate-linked heptasaccharide ($GlcNAc_2Man_5$) is produced.[9] This structure is translocated to the luminal side of the ER where three different mannosyltransferases, VI (*ALG3*), VII/IX (*ALG9*), and VIII (*ALG12*), sequentially add four mannose residues to the LLO before three different glucosyltransferases

[1]Department of Molecular Medicine and Surgery, Karolinska Institutet, Stockholm, Sweden; [2]Department of Clinical Genetics, Karolinska University Hospital, Stockholm, Sweden; [3]Experimental Pediatrics, Clinical Sciences, Lund University, Lund, Sweden; [4]Department of Clinical Chemistry, part of University Health Care in Region Skåne, Lund, Sweden; [5]Department of Pediatric Radiology, Karolinska University Hospital, Stockholm, Sweden; [6]Department of Obstetrics and Gynecology, Karolinska University Hospital, Stockholm, Sweden; [7]Department of Woman and Child Health, Karolinska Institutet, Stockholm, Sweden; [8]Centre for Inherited Metabolic Diseases, Karolinska University Hospital, Stockholm, Sweden; [9]Department of Neuropediatrics, Karolinska University Hospital, Stockholm, Sweden; [10]Section for Perinatal Pathology, Department of Pathology, Karolinska University Hospital and Karolinska Institutet, Stockholm, Sweden; [11]Department of Pediatric Imaging, Tokyo Metropolitan Children's Medical Center, Tokyo, Japan
*Correspondence: Dr G Grigelioniene, Department of Molecular Medicine and Surgery; Clinical Genetics; and Center of Molecular Medicine, Karolinska Institutet, Karolinska University Hospital, Stockholm 171 76, Sweden. Tel: +46 8 5177 3926; Fax: +46 8 327734; E-mail: Giedre.Grigelioniene@ki.se
[12]These authors contributed equally to this work.
Received 29 November 2014; Received 24 February 2015; accepted 31 March 2015

finalize the LLO with the addition of three glucose residues ($GlcNAc_2Man_9Glc_3$). ALG9 deficiency (ALG9-CDG) has been described in three patients with symptoms including intellectual disability, central hypotonia, microcephaly, epilepsy, pericardial effusion and renal cysts, but no skeletal dysplasia or visceral malformations were noted.[8,10,11]

In this report, we describe three patients with skeletal dysplasia, polycystic kidney and several multiple malformations, the phenotypes highly similar to those first reported by Gillessen-Kaesbach and Nishimura and somewhat overlapping with those of the individuals with *ALG3*- and *ALG12-CDG*.[1,2,7,12] Our patients are homozygous for a deleterious variant in the splice donor site of exon 10 in *ALG9* (NG_009210.1:g.35929T>A also denoted NM_024740.2:c.1173+2T>A). We show that this variant results in skipping of exon 10, leading to a shorter RNA with a frameshift, a premature stop codon and abnormal N-glycosylation pattern in all the affected patients.

Our study indicates that Gillessen-Kaesbach–Nishimura syndrome is caused by deleterious variants in the *ALG9* gene, thus extending the phenotypic spectrum of ALG9-CDG. In combination with previously reported similar features in few individuals with ALG3-CDG and ALG12-CDG, it suggests that Gillessen-Kaesbach–Nishimura syndrome belongs to the most severe end of the clinical spectrum associated with N-glycosylation abnormalities.

PATIENTS AND METHODS

Ethical approval

The study was approved by the Ethics Committee of the Karolinska Institutet (2014/983-31/1, 2012/2106-31/4), and written informed consent has been obtained from the parents of the patients.

Patients

Patient 1 was the third child of consanguineous parents from Turkey (Supplementary Figure S1 (A), IV:8). The couple has one healthy child and one child with molecular confirmed *de novo* Prader–Willi syndrome. A maternal uncle had three children with the paternal aunt. One of the children (Supplementary Figure S1 (A), IV:11) has an unknown congenital disease, including cardiac malformation, hypotonia, severe intellectual disability, proportionate short stature and brachycephaly. Her metabolic investigation including serum transferrin (Trf), as well as her karyotype, was unremarkable.

For patient 1, ultrasound examination at gestational age (GA) of 18 weeks according to the mother's last menstrual period demonstrated severe oligohydramnios and fetal biometry dated the pregnancy to 16 weeks. The fetal kidneys were grossly enlarged with a hyperechogenic parenchyma. Chromosome analysis of the chorionic villi biopsy demonstrated a normal fetal karyotype (46,XX). Fetal echocardiography showed a large ventricular septum defect and a double outlet right ventricle with anomalous outflow tracts. At gestational age 26+3 weeks, the mother went into spontaneous labor, and the child was stillborn following a vaginal breech delivery without any interventions due to the estimated poor prognosis associated with the diagnosed malformations.

Patients 2 and 3 were siblings from a healthy consanguineous family from Iraq (Supplementary Figure S1 (B), IV:1 and IV:2). In the first pregnancy, ultrasound scan performed at GA 19 weeks revealed brachymelia, low-set ears, micrognathia and enlarged highly echogenic kidneys with moderate hydronephrosis. Quantitative fluorescent PCR (regarding trisomy 13, 18 and 21) and array comparative genomic hybridization (array-CGH) of the chorionic villi sample were normal. Because of the severe kidney disease, the family decided to terminate the pregnancy at GA 20+1 weeks. In the second pregnancy, ultrasound at GA 18 weeks revealed similar findings as in the previous fetus. The pregnancy was terminated at GA 20 weeks.

Autopsy and sampling for genetic and biochemical analyses

All fetal autopsies were performed at the Section for Perinatal Pathology at Karolinska University Hospital in Huddinge. Skeletal surveys were performed owing to suspected skeletal dysplasia. Autopsy findings, clinical features and skeletal surveys of the three patients are summarized in Figures 1 and 2 and Tables 1 and 2. Routine examination of fetuses includes preservation of frozen tissues. Spleen specimens from the patients and age-matched controls were snap shot frozen at 80 °C at the autopsies and kept until analysis. Age-matched control samples were collected from three fetuses without internal malformations (GA 21–22 weeks) examined owing to spontaneous abortions, whereas normal spleen tissue from an adult was obtained at autopsy (approved by the Regional Ethical Committee, Lund University 2013/206). White blood cell RNA and serum from heterozygous parents and adult control individuals were used for cDNA and Trf glycosylation analyses, respectively. DNA and RNA were extracted from frozen tissue samples of spleen and lungs from the patients and from peripheral blood and saliva from the family members.

Genetic investigations

Array-CGH, whole exome sequencing (WES) and Sanger sequencing. DNA samples of patients 1 and 2 were screened for copy number variations using array-CGH with a resolution of 50 kb in combination with a custom-designed high-resolution targeted array-CGH for 872 genes involved in skeletal dysplasias, ciliary disorders and malformation syndromes (Agilent Technologies, Palo Alto, CA, USA).

WES was performed as a trio in family 1 and as a quartet in family 2 and data processing was performed at Oxford Genome Technologies (http://www.ogt.co.uk/). Briefly, paired end sequencing libraries were prepared according to the manufacturer's instruction (TruSeq, Illumina, San Diego, CA, USA), exonic sequences captured using Agilent SureSelect AllExon v4 (Agilent) and sequenced on an Illumina HiSeq 2500 instrument in high output mode (2×100 bp). Reads were mapped to the hg19 reference genome using Burrows–Wheeler Aligner, and variants were called using the Genome Analysis Toolkit as previously described.[13,14] In all, 19–29 million read pairs were obtained, with a duplication rate of 2–5% and mean target coverage of 53–66 times. Also, 94–97% of the exome target bases were covered at least 10 times. Variants were filtered for *de novo* and autosomal recessive inheritance in each family. The detected variants were further filtered by selecting those found in genes associated with clinical symptoms in the OMIM database, and variants were discarded if the phenotype in OMIM was not relevant. Further analysis was performed to discard sequencing artifacts and to predict the effect of the variant. The variant was excluded if it did not introduce a new amino acid, did not affect splicing, did not cause a frameshift or gain/loss of stop codon in a coding part of a gene. The detected variants were excluded if the gene they were identified in was not shared between the two affected fetuses from family 2 and the index patient from family 1. Filtered variants were also manually assessed using splice site prediction algorithms (SpliceSiteFinder-like, MaxEnScan, NNSPLICE, GeneSplicer and Human Splicing Finder) and pathogenicity prediction tools (SIFT, AlignGVGD, Mutation Taster and PolyPhen) integrated in the Alamut Visual tool 2.3 (Interactive Biosoftware, Rouen, France). Detected variants predicted to be causing the patients' symptoms were confirmed using Sanger sequencing (for primers, see Supplementary Table S1).

RNA isolation and cDNA analysis. RNA was extracted from 15 to 20 mg frozen spleen tissue samples and white blood cells using the RNeasy Mini Kit (QIAGEN, Hilden, Germany). First-strand cDNA was synthesized with M-MLV Reverse Transcriptase (Life Technologies, Carlsbad, CA, USA). Quality of the RNA was checked by amplification of the RNA of housekeeping gene beta-glucuronidase. cDNA was amplified and analyzed by gel electrophoresis and Sanger sequenced according to standard protocols (for primers, see Supplementary Table S1).

Homozygosity mapping. Genomic DNA from family members and the patients was analyzed using polymorphic microsatellite markers surrounding the *ALG9* gene. Markers were selected using the UCSC database (http://genome.ucsc.edu/): D11S1793, D11S1986, D11S4192, D11S4078, and D11S1987. Primers were pooled and amplified using Type-it Microsatellite PCR Kit (QIAGEN) according the the manufacturer's instructions. PCR-products were analyzed

Figure 1 Clinical phenotype of the patients 1, 2 and 3. Patient 1 (**a**, **b**, **g**); Patient 2 (**c**, **d**, **h**, **i**) patient 3 (**e**, **f**, **j**). Note phenotypic variability of the dysmorphic features but also similarities, including hypertelorism, beaked nose, hypoplastic alae nasi, micro- and retrognathia, low-set posteriorly rotated ears, short extremities with ulnar deviation of the hands and deformed feet.

using 3500xL Genetic Analyzer and GeneMapper v5 (Applied Biosystems, Thermo Fisher Scientific, Waltham, MA, USA). The results were confirmed using SNP analysis of WES data.

Analysis of Trf glycosylation in spleen samples

Approximately 2 mm^3 of dissected frozen spleen was homogenized in 200 µl of PBS, pH 7.4. The samples were centrifuged, and the supernatant was further diluted 1:4 with PBS, pH 7.4, transferred to sample vials and kept at +12 °C until analysis. A Trf immunopurification column was prepared using polyclonal anti-Trf antibodies (Dako Sweden AB, Stockholm, Sweden), which were conjugated to POROS-aldehyde self-pack medium using the manufacturer's protocol (Life Technologies Europe BV, Stockholm, Sweden). The medium was packed in empty 20 × 1 mm precolumns from IDEX (IDEX Health and Science, Wertheim-Mondfeld, Germany).

Liquid chromatography–mass spectrometry analysis of Trf. Method development and validation were performed using a Thermo Scientific Q Exactive quadrupole-orbitrap mass analyzer as previously described with minor modifications.[15] A 15-µl aliquot of each sample was applied to the immunoaffinity column in PBS (pH 7.4). Enriched Trf was eluted from the immunoaffinity column with 100 mmol/l glycine containing 2% formic acid and concentrated on an analytical C4 monolith column (Proswift RP-4H 1 × 50 mm, Thermo Fisher Scientific). The analytical C4 column was washed with water containing 1% formic acid, before a gradient was applied with increasing ratio of acetonitrile containing 1% formic acid. Trf was eluted from the C4 column at 80% acetonitrile and was introduced into the ion source. Flow rate was 200 µl/min, and total instrument acquisition time, 11 min/sample. The mass spectrometer was operated in full scan mode. Mass data were deconvoluted using Pro Mass 2.8.2 (Novatia, LLC, Newton, PA, USA).

RESULTS

Clinical features of the patients with Gillessen-Kaesbach–Nishimura syndrome

The dysmorphic features of patient 1 were more severe than in patients 2 and 3 (Figure 1). The overlapping features were retromicrognathia, thin upper lip, proptosis, hypertelorism, telecanthus, low-set posteriorly rotated ears, brachymelia of the upper extremities with ulnar deviation of the hands and polycystic kidneys. See Table 1 for summary of morphological findings in our patients and comparison with the original patients described by Gillessen-Kaesbach *et al* and Nishimura *et al*. In contrast to the facial morphology and visceral malformations, the radiographic features of our patients were more invariable. Notably, all affected fetuses shared the skeletal changes, including decreased ossification of the frontoparietal bones, thickening of the occipital bones, deficient ossification of cervical vertebral bodies and pubic bones, round pelvis and short tubular bones with metaphyseal flaring (Table 2 and Figure 2).

Screening of genomic DNA

Analysis with custom-designed high-resolution HDT array-CGH for 872 known genes involved in skeletal dysplasia, ciliary disorders and malformation syndromes did not reveal any disease-causing genetic abnormalities. Using WES, all three affected fetuses were found to be homozygous for the deleterious variant in the splice donor site of exon 10 in *ALG9* (NG_009210.1:g.35929T > A, also denoted as NM_024740.2: c.[1173+2T > A];[1173+2T > A], or hg19 chr11:g.

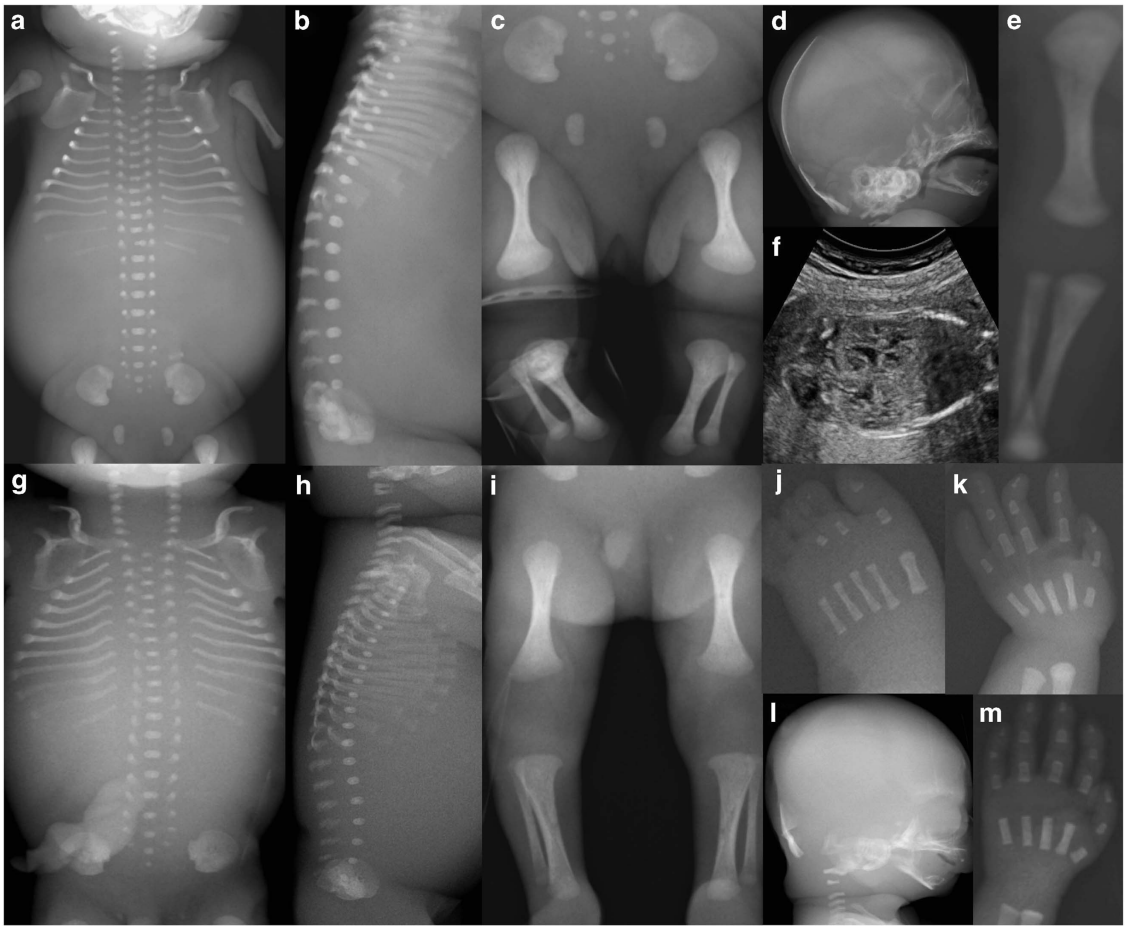

Figure 2 Radiograms and ultrasound findings. Panel of radiograms of patient 1 (GA 25+3), **a**–**e** and **j**, **k**; and patient 2 (GA 20+1) **g**–**i** and **l**, **m**. Fetal ultrasound in patient 1 (**f**). Note lack of mineralization in the vertebral bodies of the cervical spine and pubic bones and 11 pairs of short thoracic ribs (**a**, **g**), asymmetric mineralization of the 11th thoracic vertebral body (**a**), round pelvis (**a**, **c**, **g**), flat, rounded vertebral bodies in the thoracolumbar lumbar spine (**b**, **h**), shortened tubular bones with broad and rounded metaphyses (**c**, **e**, **i**), brachycephaly with thickening of the occipital bone (**d**, **l**), defective ossification of ulnar phalanges in patient 1 (**k**) but not in patient 2 (**m**) and defective ossification of toes in patient 1 (**j**). Fetal ultrasound showed polycystic kidneys in patient 1 (**f**).

[111711376T>A]. This finding was confirmed using Sanger sequencing (see Supplementary Figure S2). The healthy parents of all three patients, as well as two siblings in family 1 (IV:6, IV:7) and their cousin (IV:11) with developmental delay, were all heterozygous for this substitution. The variant was not reported in the Exome Aggregation Consortium database, Cambridge, MA, USA (URL: http://exac.broadinstitute.org), indicating the carrier frequency is <1/62 000. In addition, the variant was not found in our in-house database including 249 exomes from a local ethnically mixed population. All splicing prediction programs used indicated that the variant is likely to cause skipping of exon 10. No other homozygous, compound heterozygous or *de novo* clinically significant variants were detected in the same gene in the two families. However, in family 2, both fetuses were also homozygous for a rare variant in exon 31 of the *ANK3* gene NM_020987.3:c.2902G>C; p.(Asp968His) (hg19 chr10:g.[61874029C>G]). This variant causes a substitution at a highly conserved amino acid of the ANK3 protein in 11 species (data not shown). Pathogenic variants in the *ANK3* gene have been associated with autosomal recessive mental retardation 37.[16] The variant found in our patients was predicted to be deleterious by SIFT, AlignGVGD, Mutation Taster and PolyPhen. The parents were heterozygous carriers of this variant.

Deposition of genetic data

The data obtained in this study are submitted to ClinVar, an online gene-centered collection and display of DNA variations, with accession numbers SCV000195551 for the *ALG9* and SCV000195550 for the *ANK3* genes (http://www.ncbi.nlm.nih.gov/clinvar/).

Homozygosity mapping

Both families were consanguineous. Extended family history did not indicate a common ancestor. All affected individuals were shown to be homozygous for the same haplotype, indicating the presence of a founder pathogenic variant in both families (Supplementary Figure S1). Combined analysis of the polymorphic markers and SNPs from WES indicated that the shared homozygous region encompassed a region of 1.75–2.18 Mb, including the *ALG9* gene. None of the other genes in this region contained shared homozygous variants in the affected individuals.

Analysis of RNA splicing and *in silico* protein prediction

Primers were constructed to amplify exon–intron boundaries between exon 9, 10 and 11 (Supplementary Table S1). cDNA was amplified with a forward primer located in exon 9 in combination with a reverse primer in exon 11 specific for the transcripts that contain an extra 21

Table 1 Clinical summary and comparison of current and original patients with Gillessen-Kaesbach–Nishimura dysplasia

Study	*Current study*			*Gillessen-Kaesbach et al*[1]						*Nishimura et al*[2]	
Family and patient numbers	1-1	2-1	2-2	1-1	1-2	2-1	2-2	3-1	3-2	1	24
Patient number	1	2	3	1	2	3	4	5	6	1	2
Gender	F	M	F	F	F	M	M	M	F	F	M
Perinatal history	DAB	MA	MA	ED	MA	SB	SB	NA	ED	SB	ED
Gestational age	26	20	20	38	19	28	30	36	35	34	35
BW	1030	369	258	1428	430	1410	1800	2050	2640	2160	2000
SDS	0.8	−1.5	−2.5	−3.8	−0.7	0.7	0.6	−1.95	0.2	−0.4	−1.5
BL	30.0	23.0	21.8	35.0	26.0	35.0	39.0	NA	39.0	45.0	NA
SDS	−2.0	−1.6	−1.9	−7.4	0.0	−1.1	−0.8		−3.5	−0.2	
OFC	24.0	18.0	16.5	29.0	NA	NA	NA	NA	28.0	29.5	NA
SDS	−0.2	−1.3	−2.0	−3.7					−3.0	−1.5	
Amniotic fluid	O	N	N	NA	N	NA	NA	NA	NA	NA	P
Hydropic appearance	−	+	−	+	−	+	NA	NA	+	NA	NA
Micro/brachycephaly	+	−	−	+	+	+	+	+	+	+	+
Frontotemporal hypertrichosis	+	+	+	NA	NA	NA	NA	NA	NA	NA	NA
Anterior fontanelle	Wide	−	Wide	NA	NA	+	NA	NA	NA	Wide	Wide
Proptosis/hypertelorism	+/+	+/−	+/−	+/+	+/+	+/−	−/NA	NA	+/+	+/+	NA
Epi/telecanthus	+/+	−/−	−/−	+/+	−/+	−/+	NA/+	−/+	+	−	NA
Beaked nose/hypoplastic alae	+/+	+/+	+/+	+/+	+/+	+/+	+/+	+/NA	+/+	+	NA
Flat philtrum	+	+	+	+	+	+	+	+	+	+	NA
Micro/retrognatia	+/+	+/+	+/+	+/+	+/+	+/+	+/+	NA	+	+	NA
Low-set ears	+	+	+	+	+	+	+	+	+	+	NA
Posteriorly rotated ears	+	+	+	+	+	+	+	+	+	+	NA
Fleshy ears	+	−	−	+	−	+	+	+	NA	NA	NA
Short neck/excessive nuchal skin	+/+	+/+	+/+	+	+	+	NA	+	+	+	NA
Brachymelia	+	+	+	+	+	+	NA	+	+	+	NA
Ulnar deviation of the hands	+	+	+	+	NA	+	NA	+	+	+	NA
Abnormal feet position	+	+	+	NA	NA	+	NA	−	+	+	NA
Lung hypoplasia	+	+	+	+	+	+	+	NA	+	+	NA
Abnormal lung lobation	+	+	+	NA	NA	NA	NA	NA	NA	+	NA
Polycystic kidneys	+	+	+	+	+	+	+	+	+	Multilobular cyst	NA
Periportal fibrosis	+	−	−	+	+	+	+	NA	NA	+	NA
Pancreatic abnormalities	−	−	−	+	+	+	+	NA	NA	+	NA
Congenital heart defect	+	−	−	+	NA	+	+	NA	+	+	NA
Omphalocele	−	−	+	NA	NA	+	NA	NA	NA	−	NA
Myelo-meningocele	−	−	−	NA	NA	+	NA	NA	NA	−	NA
Uterus bicornis	+	Na	+	NA	NA	NA	NA	NA	NA	+	NA
Other features	Petechiae, hypoplasia of renal arteries, urinary bladder & ureters, atrophic ovaries	Lung/total body weight ratio 0.0096, polysplenia	Lung/ total body weight ratio 0.014, hydronephrosis normal growth plate	Genital hypoplasia		Situs inversus viscerum, anal atresia	Wide lateral ventricles of the brain, micropenis, cryptorchidism	Non-rotation of the gut		Petechiae, thrombocytopenia, migration anomaly in the cerebellum, small brain abnormal tracheal rings, diaphragmatic hernia, aniridia, camptodactyly	Thrombocytopenia, joint contractures

Abbreviations: DAB, death at birth; ED, early postnatal death; MA, medical abortion; N, normal; NA, information not available; Na, feature not applicable; O, oligohydramnios; P, polyhydramnios; SB, stillborn. Standard deviation score (SDS) for birth weight (BW, g), birth length (BL, cm) and occipitofrontal circumference (OFC, cm) calculated according to Swedish growth reference for patients older than gestational age (GA) 24 weeks and according to German growth reference for those younger than GA 24 weeks.[21,22]

Table 2 Comparison of the skeletal phenotypes of current and original patients with Gillessen-Kaesbach–Nishimura dysplasia

Study	*Current study*			*Gillessen-Kaesbach et al*[1]			*Nishimura et al*[2]	
Family and patient numbers	1-1	2-1	2-2	1-1	1-2	2-2	1	
Patient number	1	2	3	1	2	4	1	2
Thick occipital bone	+	+	+	NA	NA	NA	+	NA
Decreased ossification of the skull	+	+	+	+	+	NA	–	NA
Absent ossification of the cervical vertebral bodies	+	+	+	+	+	+	+	+
Short tubular bones	+	+	+	+	+	+	+	+
Metaphyseal broadening	+	+	+	+	NA	NA	+	+
Round pelvis	+	+	+	+	NA	NA	+	+
Absent ossification of the pubic rami	+	+	+	+	NA	NA	+	+
Shortened greater sciatic notches	+	+	+	+	NA	NA	+	+
Ovoid ischia	+	+	+	+	NA	NA	+	+

Abbreviation: NA = information not available.

nucleotides in exon 11 (corresponding to protein isoforms a/c, NP_079016.2 and NP_001071159.1, respectively). The PCR products were 106 bp in size in all three affected fetuses, whereas heterozygous parents showed fragments of 106 and 261 bp, respectively, indicating that 155 bp corresponding to exon 10 sequence were absent in the patients, that is, NM_024740.2:r.1118_1272del. The samples of control fetuses and adults showed predominance of the 261-bp fragment (Supplementary Figure S3). No fragments could be amplified from cDNA of the affected fetuses using primers located in exon 10 and 11, respectively. A normal PCR fragment size was 121/142 bp, corresponding to the two different exon 11 isoforms, and was detected in heterozygous parents and normal controls (data not shown). Subsequent sequencing of the PCR products showed that in the affected fetuses the sequence corresponding to exon 10 of the *ALG9* gene is absent, thus confirming exon skipping (Figure 3a). *In silico*-based protein prediction assay using ExPaSy tool (http://web.expasy.org/translate) shows that skipping of exon 10 causes a frameshift beginning at amino acid 340 and introducing a stop codon after 56 amino acids downstream in the major splice form a, NP_079016.2:(p.Val340Alafs*57) (Figure 3b). Comparison of the protein sequence corresponding to exon 10 in different species showed 80% conservation in *D. rerio* when compared with humans and higher conservation in other species (Supplementary Figure S4).

Glycosylation analysis

The glycosylation of Trf was analyzed using frozen spleen tissue from patients and from three age-matched controls and one adult. The ratio of mono-glycosylated, non-fucosylated to di-glycosylated, non-fucosylated Trf species was 1.5% in the adult and 2.0% in the controls. In the patients, the ratio was significantly elevated between 15 and 22.3%. (Figure 4e–h), when compared with age-matched control tissues and adult spleen (Figure 4a–d). This proves that the patients have underglycosylated Trf, indicative of a CDG. Both fetal control and patient samples had a much higher degree of fucosylation of the Trf glycans than is seen in Trf from children and adults. Serum-Trf was analyzed in the healthy heterozygous parents with normal results (data not shown).

DISCUSSION

In this study, we have identified a novel deleterious homozygous pathogenic variant at the splice donor site of exon 10 in the *ALG9* gene (NM_024740.2:c.[1173+2T>A];[1173+2T>A]) in three patients with severe skeletal dysplasia and polycystic kidney disease, combined with varying internal malformations and dysmorphic features. This splice variant leads to skipping of exon 10, causing a frameshift and prematurely truncated ALG9 protein. The features of our patients were the same as those in a lethal syndrome with skeletal dysplasia first reported by Gillessen-Kaesbach *et al* and further in detail characterized by Nishimura *et al*.[1,2] This indicates that Gillessen-Kaesbach–Nishimura syndrome belongs to a group of CDG.

The *ALG9* gene has two different 5′ untranslated regions and exon 11 can be spliced at two sites that differ by 21 bp, resulting in four major ALG9 isoforms. The sequence encoded by the exon 10 of *ALG9* contains a highly evolutionarily conserved stretch of amino acids that is present in all α2/α6 mannosyltransferases in humans and down to *S. cerevisiae* and is important for the mannose acceptor site of the enzyme.[17] The skipping of exon 10 in our patients is predicted to result in a truncated ALG9 protein lacking these conserved amino acids as well as three putative transmembrane domains and the ER-retention signal located at the C-terminal end of the protein. We conclude that the homozygous variant NM_024740.2: c.1173+2T>A in the *ALG9* gene is thus likely to result in a nonfunctional enzyme. To gather biochemical proof of deficient N-glycosylation, serum Trf is usually analyzed. For our patients, no serum samples or viable tissues were available. We therefore analyzed Trf obtained from frozen spleen extracts from all three fetuses. First, we showed that analysis of spleen-derived Trf from adults nicely matched the profile of serum Trf, where the Trf molecules were almost exclusively modified with two complex biantennary N-linked chains (Supplementary Figure S5). Furthermore, the Trf species from fetal control tissue also carry two such chains to a large extent, with a ratio of mono-/di-glycosylated species of Trf of 2%, which corresponds to normal reference levels in adult serum. On the other hand, in the three patients, underglycosylation of Trf was significant, with a ratio of mono-/di-glycosylated species of 15–22%. Of note, the fetal Trf-derived glycans were to a large degree modified with fucose, which is in accordance with a study of Trf derived from amniotic fluid,[18] thus suggesting that overfucosylation of Trf occurs normally in the fetus.

The predicted truncated ALG9 lacks the mannose acceptor, three transmembrane domains and the ER-retention signal. This very likely leads to a severely decreased enzyme function and therefore one might expect the underglycosylation of transferrin to be even more pronounced. However, an attractive explanation to our data in this context is based on a paper by Vleugels *et al*.[11] They show that fibroblasts from an ALG9-CDG patient accumulate the two LLO acceptors of the ALG9 mannosyltransferase (Man8GlcNa2 and Man6-GlcNAc2) and that these LLOs are efficiently transferred to protein by the oligosaccharyltransferase. As protein-bound oligosaccharides, they

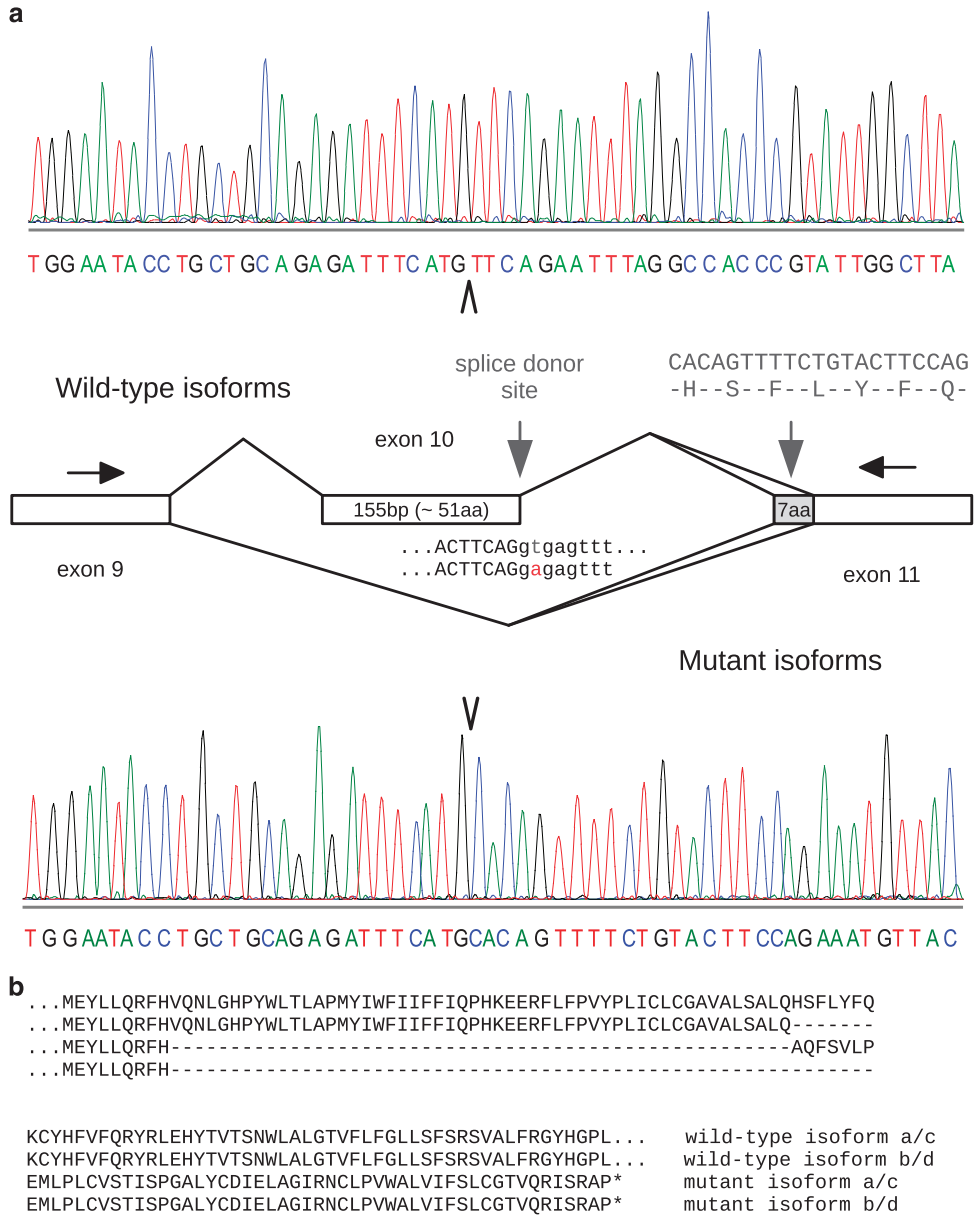

Figure 3 Diagram including results of exon 10 skipping in cDNA sequencing (**a**) and *in silico* prediction of its consequences at the protein level (**b**). (**a**) Note that *ALG9* exon 11 has two alternative splice isoforms, which differ by 21 nucleotides. Vertical arrowheads show boundaries between exons 9 and 10 and exons 9 and 11 in wild-type and mutated cDNA, respectively. (**b**) Skipping of exon 10 leads to a frameshift after amino acid 340 in the predicted protein sequence, resulting in a truncated protein.

act as substrates for glucosylation and partake in regulation of protein degradation by the ER-associated degradation system.[11] Some symptoms in CDG may thus not be directly due to underglycosylation but rather due to dysglycosylation leading to, for example, an increased glycoprotein degradation and ER stress. When protein bound, these two LLOs can also be further de-mannosylated in the *cis*-Golgi and complex chains can be formed by the addition of GlcNAc, Gal and NeuAc in the *cis* through *trans*-Golgi compartments.[19] The transfer of the two LLOs is, however, probably not as efficient as the transfer of full-length LLO, as reflected by the detected underglycosylation despite this salvage pathway.

In most CDG type I cases, the profile also contains a significant amount of non-glycosylated Trf, which was not found in our patients. Interestingly, one of the ALG9-CDG patients published previously also had a similar profile showing that presence of non-glycosylated Trf is not a prerequisite for the diagnosis of ALG9-CDG.[7] In accordance with the notion that the CDGs are recessive disorders and that the capacity of the LLO biosynthetic machinery can cope with haploinsufficiency, we found no signs of underglycosylation in the parental serum (data not shown).

Three patients with homozygous missense variants in *ALG9* were previously reported. By analyzing *ALG9* cDNA, Frank *et al*[8] reported one patient with p.Glu523Lys, which corresponds to HGVS nomenclature: NM_024740.2:c.1588G>A, p.Glu530Lys, rs121908022. The other two patients, described by Weinstein *et al*[10] and Vleugels *et al*[11] had p.(Tyr286Cys), which corresponds

to HGVS nomenclature: NM_024740.2:c.860A>G, p.(Tyr287Cys), rs121908023. Their clinical features were different from our patients and included microcephaly, central hypotonia, seizures, psychomotor retardation, diffuse brain atrophy with delayed myelination, failure to thrive, bronchial asthma, pericardial effusion, hepatosplenomegaly and esotropia; the main overlapping feature with our patients was polycystic kidney disease.[8,10,11] There was no reference to the phenotypic details regarding facial features or skeletal abnormalities in the previous reports.[8,10,11] It is possible that the milder phenotypes of the previously reported patients with ALG9-CDG may be explained by residual function of the enzyme containing pathogenic missense variants. In fact, partial enzyme deficiency in the patient with p.Glu530Lys was ascertained based on the yeast complementation assay and presence of the normal N-linked oligosaccharides ($GlcNAc_2Man_8$, $GlcNAc_2Man_9$ and $GlcNAc_2Man_9Glc_1$) in addition to abnormal $GlcNAc_2Man_6$ in 3H-labeled fibroblast-derived glycoproteins.[8]

The skeletal abnormalities, facial features as well as the pattern of visceral malformations of the original patients with Gillessen-Kaesbach–Nishimura syndrome and our patients in this study partially overlap with the phenotype of those with ALG3- and ALG12-CDG. These three mannosyltransferases VI (ALG3), VII/IX (ALG9) and VIII (ALG12) function in direct sequential order, adding mannose moieties to the growing LLO in the ER, therefore it is not surprising to discover that loss-of-function variants in these genes can result in overlapping phenotypes (Supplementary Table S2). N-glycosylation is tissue

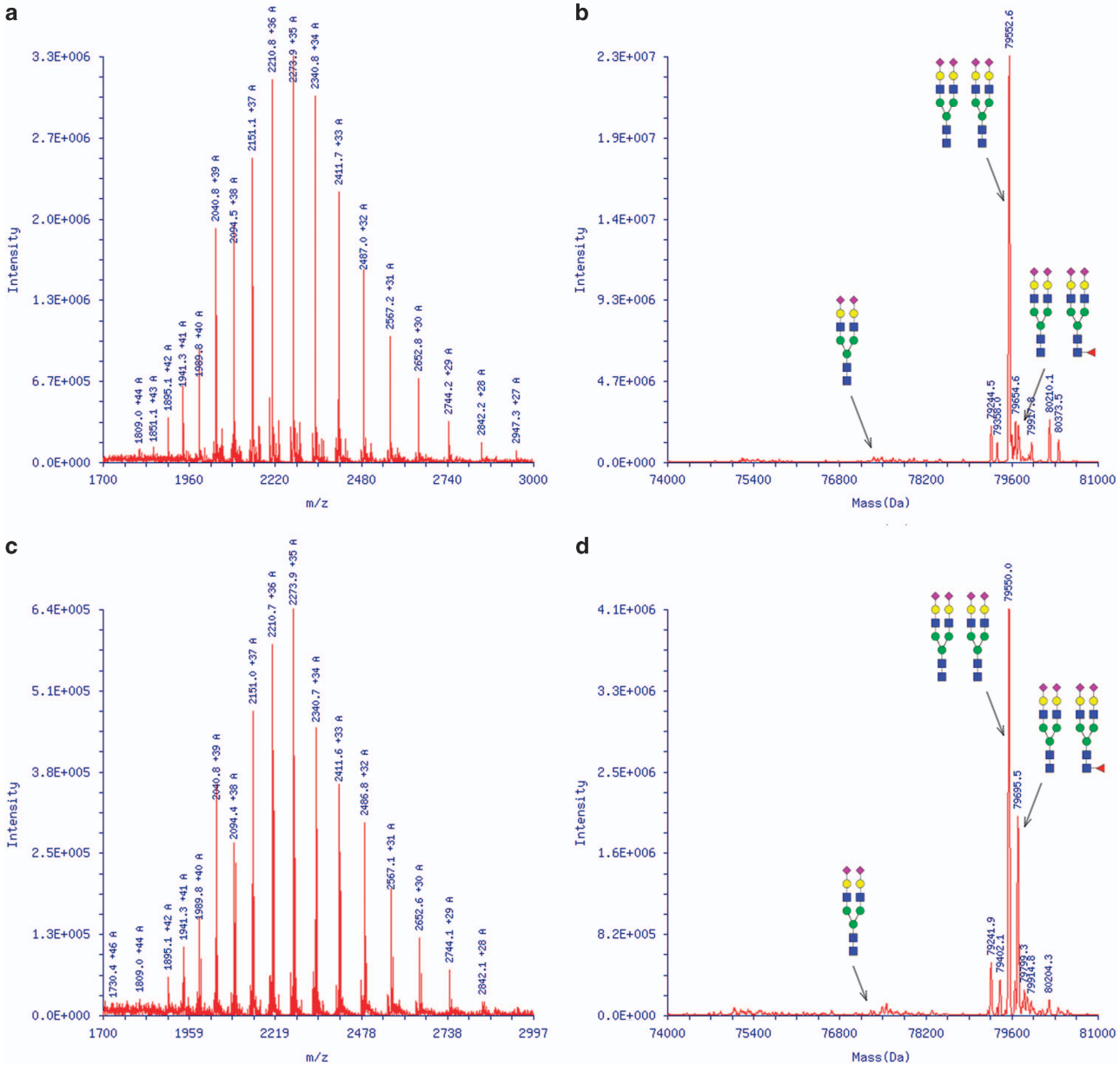

Figure 4 Mass spectra of affinity-purified Trf before (**a**, **c**, **e**, **g**) and after deconvolution (**b**, **d**, **f**, **h**). The structures of the oligosaccharides represented by the masses are indicated (blue squares = GlcNAc; green circles = Man; yellow circles = galactose; purple diamonds = sialic acid; red triangles = fucose). Panels **a**/**b**; representative mass data of Trf from the spleen obtained from an adult individual. Panels **c**/**d**; representative data from spleen samples from control fetuses. Panel **e**/**f** and **g**/**h**; representative data from spleen samples from affected fetuses, showing an abnormal peak of underglycosylated Trf.

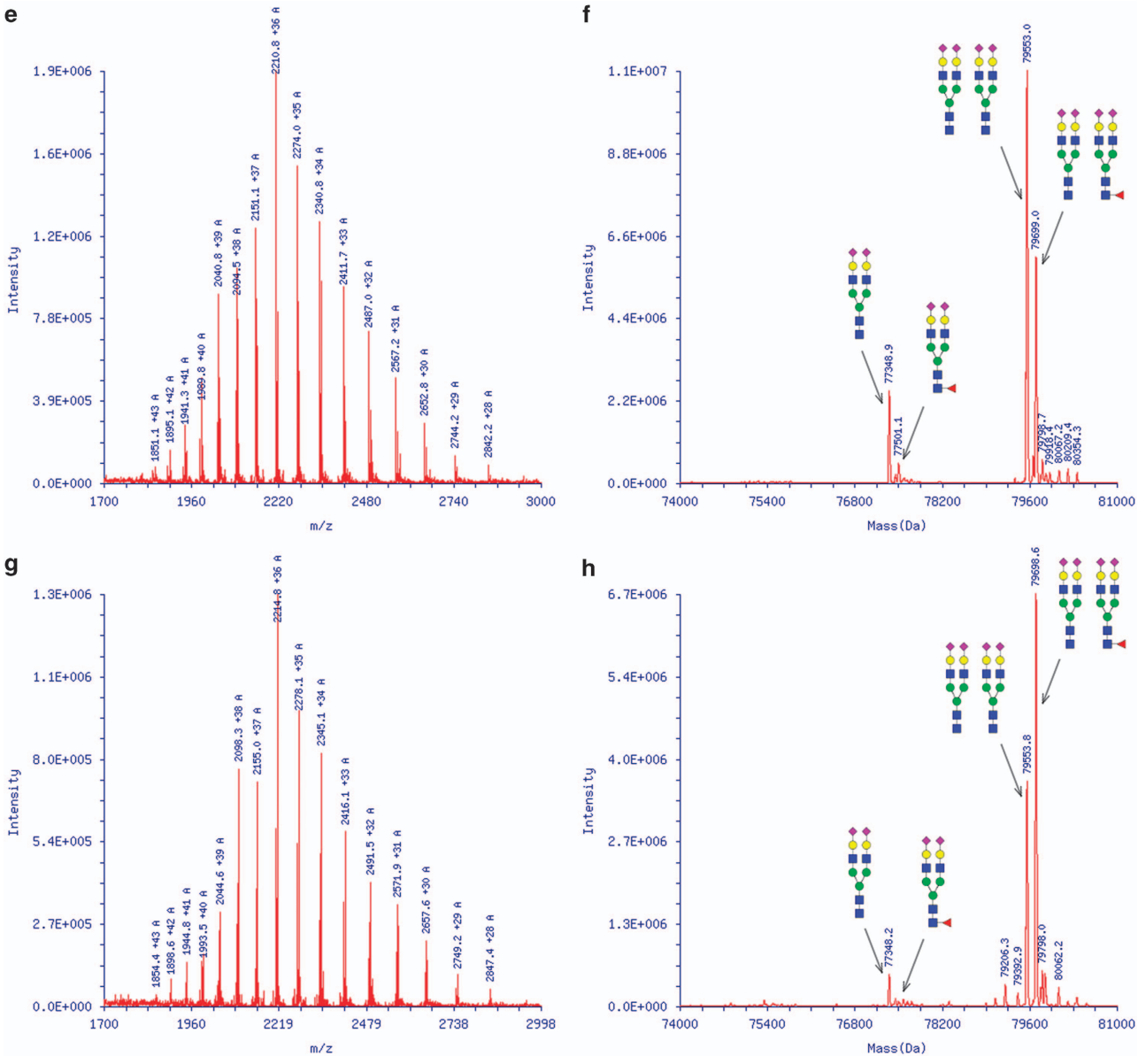

Figure 4 Continued.

specific and is required for the correct function of >2300 proteins (mainly transporters, receptors and carbohydrate-binding proteins) in mouse.[20] Thus defects in N-glycosylation would be expected to give rise to a myriad of symptoms from various organs with varying expressivity.

Extended family history of the studied pedigrees, originating from Turkey and Iraq, respectively, did not indicate a common ancestor. All affected individuals were shown to be homozygous for a common region of approximately 2 Mb including the *ALG9* gene, suggesting the presence of a common founder variant in the Middle East.

Furthermore, in family 2, both fetuses had a homozygous probably disease-causing rare variant in the *ANK3* gene. The parents were heterozygous carriers. Pathogenic variants in the *ANK3* gene have been associated with autosomal recessive mental retardation 37.[16] Neither skeletal dysplasia nor dysmorphic features were reported in the patients with autosomal mental retardation type 37,[16] indicating that the homozygous *ANK3* variant most likely does not contribute to the congenital malformations in family 2.

In summary, this study extends the ALG9-CDG phenotypic spectrum, including features of severe skeletal dysplasia, visceral malformations and facial dysmorphic features. Mass spectrometry is a helpful tool in the diagnostic process, and we show that lack of preserved serum from the fetal patients could be overcome by analyzing Trf obtained from frozen spleen samples, allowing for the confirmation/exclusion of CDG in postmortal samples. The most severe cases of early N-glycosylation disorders have overlapping phenotypes with skeletal dysplasia, visceral malformations and dysmorphic features, showing that CDG is an important differential diagnosis in fetal lethal malformation syndromes.

CONFLICT OF INTEREST

The authors declare no conflict of interest.

ACKNOWLEDGEMENTS

We thank our patients and their families for participating in this study, Professor Magnus Nordenskjöld for generous support and nice environment at

the laboratory and Professor Matthew Warman for advice regarding this manuscript. We also thank laboratory engineers and technicians Isabel Neira, Weini Tadesse, Malin Hertzman, Anette Niklasson, Annica Westlund, Christine Carlsson-Skwirut, Britt Masironi and Nina Jäntti for assistance. GG, AN and ET have been supported through the regional agreement on medical training and clinical research (ALF) between Stockholm County Council (531315) and Karolinska Institutet, by grants from Kronprinsessan Lovisa and Axel Tiellmans Minnesfond, Stiftelsen Samariten, Frimurare Barnhuset i Stockholm, Karolinska Institutet, Promobilia Foundation and The Swedish Childhood Cancer Foundation. EAE received grants from the Crafoord Foundation and Kungl. Fysiografiska Sällskapet in Lund.

1 Gillessen-Kaesbach G, Meinecke P, Garrett C *et al*: New autosomal recessive lethal disorder with polycystic kidneys type Potter I, characteristic face, microcephaly, brachymelia, and congenital heart defects. *Am J Med Genet* 1993; **45**: 511–518.
2 Nishimura G, Nakayama M, Fuke Y *et al*: A lethal osteochondrodysplasia with mesomelic brachymelia, round pelvis, and congenital hepatic fibrosis: two siblings born to consanguineous parents. *Pediatr Radiol* 1998; **28**: 43–47.
3 Jaeken J: Congenital disorders of glycosylation (CDG): it's (nearly) all in it!. *J Inherit Metab Dis* 2011; **34**: 853–858.
4 Freeze HH, Eklund EA, Ng BG *et al*: Neurology of inherited glycosylation disorders. *Lancet Neurol* 2012; **11**: 453–466.
5 Coman D, Irving M, Kannu P *et al*: The skeletal manifestations of the congenital disorders of glycosylation. *Clin Genet* 2008; **73**: 507–515.
6 Murali C, Lu JT, Jain M *et al*: Diagnosis of ALG12-CDG by exome sequencing in a case of severe skeletal dysplasia. *Mol Genet Metab Rep* 2014; **1**: 213–219.
7 Kranz C, Basinger AA, Gucsavas-Calikoglu M *et al*: Expanding spectrum of congenital disorder of glycosylation Ig (CDG-Ig): sibs with a unique skeletal dysplasia, hypogammaglobulinemia, cardiomyopathy, genital malformations, and early lethality. *Am J Med Genet A* 2007; **143A**: 1371–1378.
8 Frank CG, Grubenmann CE, Eyaid W *et al*: Identification and functional analysis of a defect in the human ALG9 gene: definition of congenital disorder of glycosylation type IL. *Am J Hum Genet* 2004; **75**: 146–150.
9 Freeze HH, Chong JX, Bamshad MJ *et al*: Solving glycosylation disorders: fundamental approaches reveal complicated pathways. *Am J Hum Genet* 2014; **94**: 161–175.
10 Weinstein M, Schollen E, Matthijs G *et al*: CDG-IL: an infant with a novel mutation in the ALG9 gene and additional phenotypic features. *Am J Med Genet A* 2005; **136**: 194–197.
11 Vleugels W, Keldermans L, Jaeken J *et al*: Quality control of glycoproteins bearing truncated glycans in an ALG9-defective (CDG-IL) patient. *Glycobiology* 2009; **19**: 910–917.
12 Sun L, Eklund EA, Chung WK *et al*: Congenital disorder of glycosylation id presenting with hyperinsulinemic hypoglycemia and islet cell hyperplasia. *J Clin Endocrinol Metab* 2005; **90**: 4371–4375.
13 Li H, Durbin R: Fast and accurate short read alignment with Burrows-Wheeler transform. *Bioinformatics* 2009; **25**: 1754–1760.
14 DePristo MA, Banks E, Poplin R *et al*: A framework for variation discovery and genotyping using next-generation DNA sequencing data. *Nat Genet* 2011; **43**: 491–498.
15 Lacey JM, Bergen HR, Magera MJ *et al*: Rapid determination of transferrin isoforms by immunoaffinity liquid chromatography and electrospray mass spectrometry. *Clin Chem* 2001; **47**: 513–518.
16 Iqbal Z, Vandeweyer G, van der Voet M *et al*: Homozygous and heterozygous disruptions of ANK3: at the crossroads of neurodevelopmental and psychiatric disorders. *Hum Mol Genet* 2013; **22**: 1960–1970.
17 Oriol R, Martinez-Duncker I, Chantret I *et al*: Common origin and evolution of glycosyltransferases using Dol-P-monosaccharides as donor substrate. *Mol Biol Evol* 2002; **19**: 1451–1463.
18 van Rooijen JJ, Jeschke U, Kamerling JP *et al*: Expression of N-linked sialyl Le(x) determinants and O-glycans in the carbohydrate moiety of human amniotic fluid transferrin during pregnancy. *Glycobiology* 1998; **8**: 1053–1064.
19 Stanley P, Schachter H, Taniguchi N: *Essentials of Glycobiology*. NY, USA: Cold Spring Harbor Laboratory Press, 2009.
20 Zielinska DF, Gnad F, Wisniewski JR *et al*: Precision mapping of an in vivo N-glycoproteome reveals rigid topological and sequence constraints. *Cell* 2010; **141**: 897–907.
21 Niklasson A, Albertsson-Wikland K: Continuous growth reference from 24th week of gestation to 24 months by gender. *BMC Pediatr* 2008; **8**: 8.
22 Voigt M, Fusch C, Olbertz D *et al*: Analyse des neugeborenenkollektivs der bundesrepublik deutschland. *Geburtsh Frauenheilk* 2006; **66**: 956–970.

Supplementary Information accompanies this paper on European Journal of Human Genetics website (http://www.nature.com/ejhg)